Regular Article

IMMUNOBIOLOGY

Janus kinase inhibition lessens inflammation and ameliorates disease in murine models of hemophagocytic lymphohistiocytosis

Rupali Das,[1] Peng Guan,[2,*] Leslee Sprague,[2,*] Katherine Verbist,[3] Paige Tedrick,[3] Qi Angel An,[4] Cheng Cheng,[4] Makoto Kurachi,[5] Ross Levine,[6] E. John Wherry,[5] Scott W. Canna,[7] Edward M. Behrens,[7] and Kim E. Nichols[3]

[1]Department of Physiology, Michigan State University, East Lansing, MI; [2]Division of Oncology, Children's Hospital of Philadelphia, Philadelphia, PA; [3]Department of Oncology and [4]Department of Biostatistics, St. Jude Children's Research Hospital, Memphis, TN; [5]Department of Microbiology, Institute for Immunology, University of Pennsylvania, Philadelphia, PA; [6]Department of Oncology, Memorial Sloan Kettering Cancer Center, New York, NY; and [7]Division of Rheumatology, The Children's Hospital of Philadelphia, Philadelphia, PA

Key Points

- Ruxolitinib treatment lessens immunopathology and prolongs survival in murine models of hemophagocytic lymphohistiocytosis.
- In vivo exposure to ruxolitinib limits CD8$^+$ T-cell expansion and proinflammatory cytokine production.

Hemophagocytic lymphohistiocytosis (HLH) comprises an emerging spectrum of inherited and noninherited disorders of the immune system characterized by the excessive production of cytokines, including interferon-γ and interleukins 2, 6, and 10 (IL-2, IL-6, and IL-10). The Janus kinases (JAKs) transduce signals initiated following engagement of specific receptors that bind a broad array of cytokines, including those overproduced in HLH. Based on the central role for cytokines in the pathogenesis of HLH, we sought to examine whether the inhibition of JAK function might lessen inflammation in murine models of the disease. Toward this end, we examined the effects of JAK inhibition using a model of primary (inherited) HLH in which perforin-deficient (*Prf1*$^{-/-}$) mice are infected with lymphocytic choriomeningitis virus (LCMV) and secondary (noninherited) HLH in which C57BL/6 mice receive repeated injections of CpG DNA. In both models, treatment with the JAK1/2 inhibitor ruxolitinib significantly lessened the clinical and laboratory manifestations of HLH, including weight loss, organomegaly, anemia, thrombocytopenia, hypercytokinemia, and tissue inflammation. Importantly, ruxolitinib treatment also significantly improved the survival of LCMV-infected *Prf1*$^{-/-}$ mice. Mechanistic studies revealed that in vivo exposure to ruxolitinib inhibited signal transducer and activation of transcription 1–dependent gene expression, limited CD8$^+$ T-cell expansion, and greatly reduced proinflammatory cytokine production, without effecting degranulation and cytotoxic function. Collectively, these findings highlight the JAKs as novel, druggable targets for mitigating the cytokine-driven hyperinflammation that occurs in HLH. These observations also support the incorporation of JAK inhibitors such as ruxolitinib into future clinical trials for patients with these life-threatening disorders. (*Blood*. 2016;127(13):1666-1675)

Introduction

Hemophagocytic lymphohistiocytosis (HLH) comprises a genetically heterogeneous group of disorders characterized by a highly stimulated but ineffective immune response.[1] In HLH, activated T cells and macrophages accumulate in organs such as the liver, spleen, bone marrow, and brain, where they copiously secrete cytokines and mediate significant tissue damage.[2] The standard approach to treatment involves the administration of broadly immunosuppressive and cytotoxic agents, such as high-dose steroids and etoposide[3,4] often followed by allogeneic stem cell transplantation. For patients whose disease fails to respond or relapses while on treatment, there are few effective salvage therapies and the fatality rate can reach up to 50% or higher.[4,5]

"Primary" HLH occurs as a hereditary condition due to the presence of biallelic inactivating germline mutations in 1 of several genes involved in lymphocyte cytotoxic function, including *PRF1*, *UNC13D*, *STX11*, and *STXBP2*.[1] Due to these mutations, patients with primary HLH exhibit markedly reduced or absent natural killer (NK) and CD8$^+$ T-cell cytotoxicity. Under normal circumstances, NK and CD8$^+$ T cells kill pathogen-infected cells as well as activated antigen-presenting cells to promote immunoregulation and termination of the immune response.[6,7] Indeed, perturbations in these cytotoxicity-dependent functions have been shown to underlie the recurrent bouts of hyperinflammation that typify primary HLH. In "secondary" HLH, patients lack underlying genetic mutations,[1] yet they experience hyperinflammation in the setting of certain infections, malignancies, or autoimmune disorders. Recently, a cytokine release syndrome resembling HLH has also been described in patients receiving T-cell–based cancer immunotherapies, including blinatumumab[8] and chimeric antigen receptor-modified T cells.[9]

Many of the key cytokines contributing to inflammation in HLH, including interferon-γ (IFNγ) and interleukins 2 and 6 (IL-2 and IL-6), bind to receptors that signal via the Janus kinases (JAKs; JAK1-3, Tyk2).[10] Upon cytokine binding, 1 or more JAKs come into proximity with the cytokine receptors, where they phosphorylate tyrosine residues within the receptor tails. These phosphorylated residues then become

Submitted December 4, 2015; accepted January 13, 2016. Prepublished online as *Blood* First Edition paper, January 29, 2016; DOI 10.1182/blood-2015-12-684399.

*P.G. and L.S. contributed equally to this work.

The online version of this article contains a data supplement.

There is an Inside *Blood* Commentary on this article in this issue.

The publication costs of this article were defrayed in part by page charge payment. Therefore, and solely to indicate this fact, this article is hereby marked "advertisement" in accordance with 18 USC section 1734.

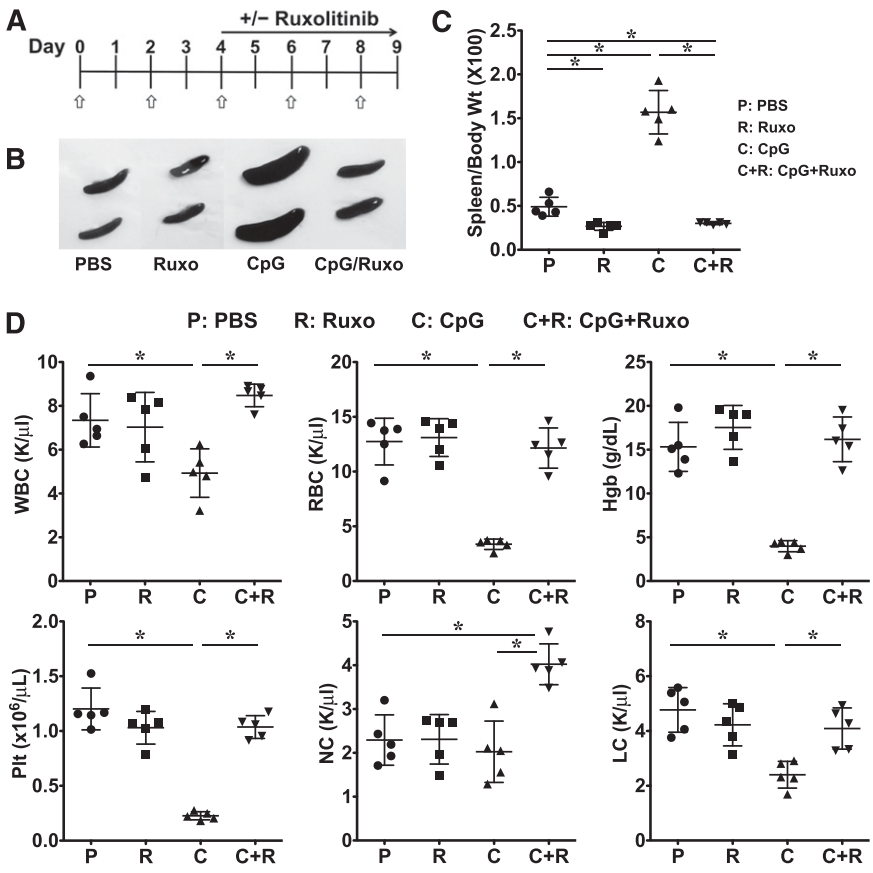

Figure 1. Treatment with ruxolitinib lessens CpG-induced splenomegaly and cytopenias. (A) C57BL/6 (B6) mice were treated with PBS or CpG (50 μg) every other day as indicated (open/white arrow). Beginning on day 4, mice did or did not receive ruxolitinib (Ruxo) twice daily by oral gavage. On day 9, mice were euthanized and analyses performed. (B) Whole-spleen images from treatment groups. (C) Splenomegaly was quantified by measuring the ratio of spleen to body weight × 100. (D) Blood was analyzed for WBCs, RBCs, hemoglobin, platelets, neutrophils (NC), and lymphocytes (LC). Individual symbols each depict 1 mouse with horizontal lines representing the mean ± standard deviation (SD). Data are representative of 3 independent experiments. *$P < .05$.

binding sites for the signal transducer and activation of transcription (STAT) family of transcription factors, which are themselves phosphorylated by the active JAKs. Subsequent STAT phosphorylation results in homo- or heterodimerization, translocation to the nucleus, and regulation of numerous downstream target genes.[10]

Based on their essential roles in transmitting cytokine-induced signals, the JAKs have become a target for pharmacologic manipulation in inflammatory diseases.[11-13] Accordingly, studies have shown that JAK inhibition reduces the signs and symptoms of rheumatoid arthritis and ulcerative colitis,[14,15] as well as the myeloproliferative disorders.[16,17] Given the efficacy of JAK inhibition in these other conditions, we hypothesized that JAK inhibition might serve as a valid therapeutic approach in HLH. To test this hypothesis, we examined the effects of JAK inhibition using murine models of primary and secondary HLH. Notably, treatment with the JAK1/2 inhibitor ruxolitinib significantly reduced disease manifestations and enhanced survival in both murine models. Ruxolitinib diminished $CD8^+$ T-cell accumulation and cytokine production, while sparing degranulation and cytotoxicity. Collectively, these data provide rationale for the incorporation of ruxolitinib or similar JAK inhibitors into future clinical trials to improve the outcomes for patients with HLH.

Methods

Mice

C57BL/6 (B6) and *Prf1*$^{-/-}$ mice were from The Jackson Laboratory (Bar Harbor, ME). Experiments were performed with approval of the Institutional Animal Care and Use Committees at The Children's Hospital of Philadelphia and St. Jude Children's Research Hospital.

CpG-induced model of secondary HLH

B6 mice were injected with 50 μg of CpG DNA on days 0, 2, 4, 6, and 8 as described.[18] Mice were treated or not with ruxolitinib (90 mg/kg; INCB018424; Selleck Chemicals, Houston, TX) twice daily by oral gavage starting on day 4. This dose results in a peak serum level of 3 to 4 μM, which is similar to a 25-mg oral dose in humans (R.L., unpublished observation, May 2015). Ruxolitinib was prepared in citrate buffer (pH 3.5) with 20% (wt/vol) Captisol (Ligand Pharmaceuticals, La Jolla, CA). Mice were euthanized and organs collected for analysis on day 9.

LCMV-induced model of primary HLH

Prf1$^{-/-}$ mice were infected with 2×10^5 plaque-forming units (PFUs) lymphocytic choriomeningitis virus (LCMV) Armstrong by intraperitoneal injection on day 0. Starting on day 4 postinfection, mice were treated or not with ruxolitinib (90 mg/kg) twice daily by oral gavage. Mice were euthanized and organs collected and evaluated between days 8 and 10 postinfection.

Antibodies and other reagents

Fluorochrome-conjugated anti-mouse CD4, CD8, CD25, B220, CD69, CD107a, IFNγ, NK1.1, T-cell receptor β, and CD11c monoclonal antibodies were from BD Biosciences (San Jose, CA). Anti-mouse CD44, tumor necrosis factor α (TNFα), and IL-2 were from eBioscience (San Diego, CA). Allophycocyanin-conjugated D^b glycoprotein 33 (gp33) tetramer was from E.J.W. (University of Pennsylvania, Philadelphia, PA).

Flow cytometry

Cell suspensions from blood, liver, and spleen were stained using standard protocols and subjected to multicolor flow cytometry using an LSR II flow

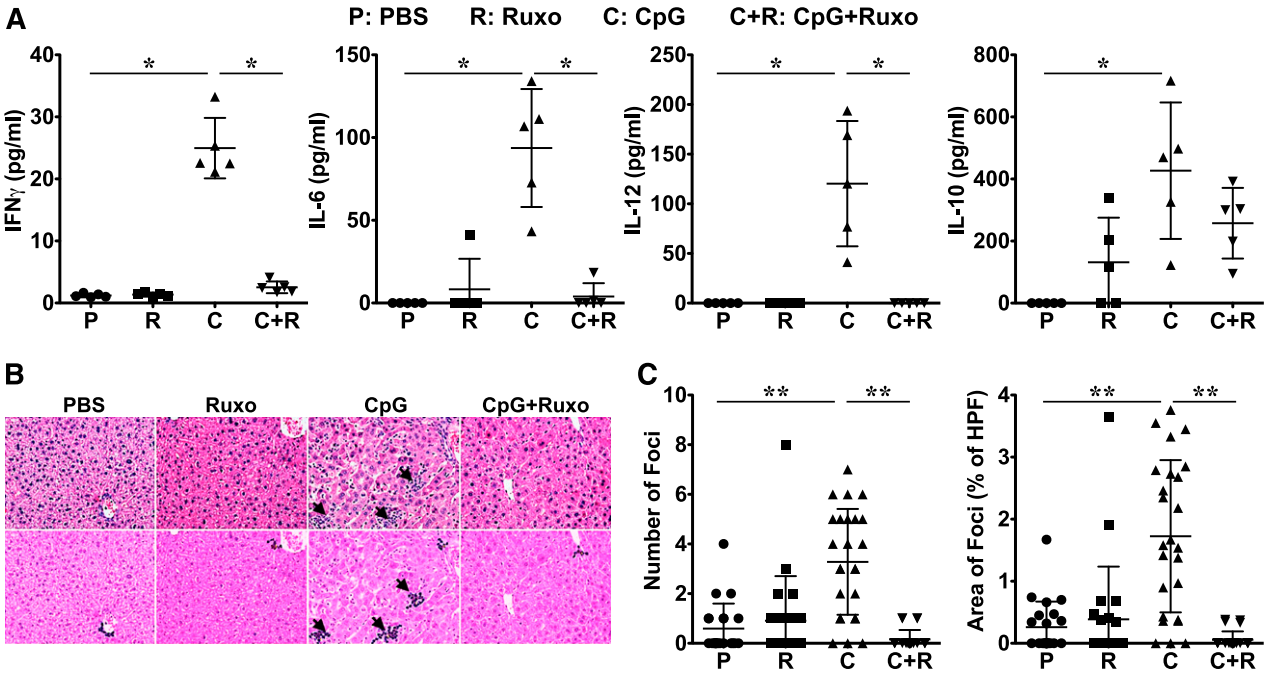

Figure 2. Ruxolitinib treatment reduces CpG-induced hypercytokinemias and ameliorates liver inflammation. (A) Serum cytokine levels were assessed on day 9. (B) H&E-stained liver sections demonstrate inflammatory infiltrates (dark purple clusters), indicated by arrows. Representative sections are shown at a magnification of ×20 (top panels) and following computer analysis of inflammatory area (bottom panels). (C) The number of inflammatory foci (left) and percent area occupied by inflammatory foci with respect to the high-power field (HPF) of view (right) was determined by computer analysis of histologic samples. Symbols in panel A represent individual mice in each treatment group where in panel C they represent the number of, or area encompassed by, inflammatory foci (clusters containing >8 lymphocytes) per ×20 field of view. Data shown are mean ± SD and are representative of 3 independent experiments. $^{*}P < .05$; $^{**}P < .001$.

cytometer (BD Biosciences). Analysis was carried out using Flow Jo version 9.6.4 (Tree Star, Ashland, OR).

Analyses of serum cytokine levels

Enzyme-linked immunosorbent assay kits to detect IL-6, IL-10, IL-12, IFNγ, and TNFα were purchased from BD Biosciences (San Diego, CA). All kits were used according to the manufacturer's protocols.

Histology

Livers were fixed in 10% formalin (wt/vol) (Fisher Scientific, Fair Lawn, NJ), embedded in paraffin, cut into 5-μM sections, and stained with hematoxylin and eosin (H&E). Images were captured using a Nikon Eclipse 90i equipped with a Nikon DS-Fi1 camera and NIS-Elements BR 3.0 software (Nikon, Japan). For each sample, 5 random fields were captured at ×20 magnification (Nikon Plan Apo 10×; NA 0.45) and subjected to computer-based quantification of inflammatory infiltrates using the BZ-II Analyzer Hybrid Cell Count software (Keyence, Japan). The number of inflammatory foci (clusters containing >8 lymphocytes) was determined, along with the area of the inflammatory infiltrate (relative to the field of view).

In vitro restimulation assay

Splenocytes were incubated at 37°C (5% CO_2) at 1×10^7 cells per mL for 5 hours with or without gp33-41 (0.4 ng/μL) or gp61-80 peptide (1 ng/μL) in complete RPMI 1640 (RPMI, 1% sodium pyruvate, 1% penicillin-streptomycin-glutamine, 10% fetal bovine serum [FBS]). BD GolgiStop, BD GolgiPlug, and phycoerythrin-conjugated anti-CD107a antibody (BD Biosciences) were added directly to the medium. LCMV gp33-41 and gp61-80 peptides were from AnaSpec (Fremont, CA). Cells were then washed in cold phosphate-buffered saline (PBS) with 1% FBS, and stained for intracellular IFNγ, TNFα, and IL-2 using the Cytofix/Cytoperm Kit following the manufacturer's protocol (BD Biosciences).

Assessment of viral titer

Vero cells were plated in 6-well dishes at 1×10^5 cells per mL in modified Eagle medium with 10% serum, 1% penicillin, 1% streptomycin, 1% L-glutamine, and incubated overnight at 37°C. Cells were then incubated with 200 μL of a 10-fold serial dilution of liver lysates for 1 hour at 37°C, and overlaid with a 1:1 mixture of 1% agarose and 2× 199 medium (Corning Life Sciences, Tewskbury, MA) with 10% FBS. Plates were incubated at 37°C for 4 days. Wells were then overlaid with 2 mL of a 1:1 mixture of 1% agarose and 2× 199 medium with 1:20 neutral red. Plates were incubated at 37°C for 12 more hours and plaques counted to determine the PFU per gram of tissue.

Cytotoxicity assay

Splenocytes from ruxolitinib-treated or untreated B6 mice were obtained 8 days post-LCMV infection. $CD8^+CD44^+$ T cells were sort-purified using a MoFlow Astrios cell sorter (Beckman Coulter, Fullerton, CA). EL4 target cells were incubated or not with 20 μM gp33 peptide for 3 hours, and then labeled with 100 μCi ^{51}Cr (Na_2CrO_4; Perkin Elmer; Waltham, MA). ^{51}Cr-labeled targets and effectors were washed in complete RPMI, plated in triplicate at varying effector-to-target (E:T) ratios, and incubated for 5 hours at 37°C (5% CO_2). Supernatants were collected and radioactivity measured to determine the percent-specific lysis as described.[19]

Gene expression profiling

On day 8 postinfection, splenic $CD8^+$ T cells were sorted into lysis buffer (Qiagen, Valencia, CA) and RNA isolated. Complementary DNA was prepared and hybridized to the mouse Affymetrix ST 2.0 Chip. The array data set was modeled using a 2-way comparison of untreated vs ruxolitinib-treated mice and uninfected vs infected mice. Principal component analysis (PCA) was performed on unfiltered data using Partek Genomics Suite (St. Louis, MO). Unsupervised hierarchical clustering was performed on probe sets filtered by a log2 difference >1.5. Genome-wide significant probe sets (with a false discovery rate <0.05 via Benjamini-Hochberg correction) identified by comparing LCMV-infected/untreated or LCMV-infected/ruxolitinib-treated mice were

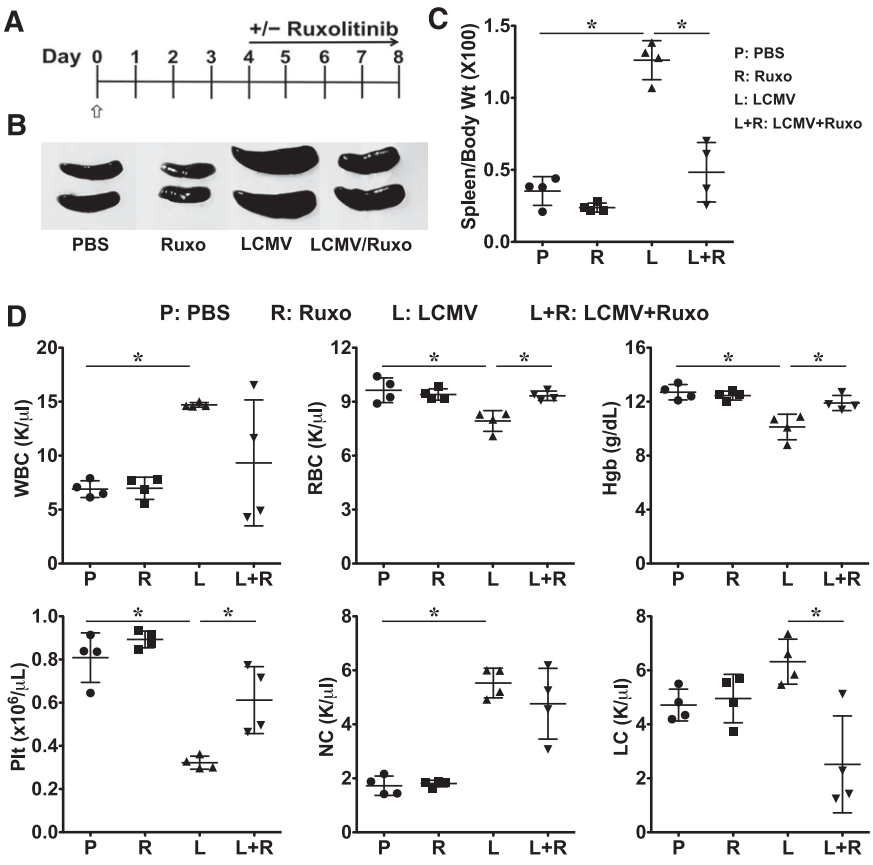

Figure 3. Treatment with ruxolitinib improves laboratory features of HLH in LCMV-infected *Prf1*$^{-/-}$ mice. (A) *Prf1*$^{-/-}$ mice were infected with 2×10^5 PFU LCMV on day 0 (open/white arrow). Starting on day 4, mice were treated or not with ruxolitinib twice daily by oral gavage. Between days 8 and 10, mice were euthanized and analyses performed. (B) Whole-spleen images from treatment groups. (C) Splenomegaly was quantified by measuring the ratio of spleen to body weight × 100. (D) Blood was analyzed for the number of WBCs, RBCs, Hgb, Plt, NCs, and LCs. Data shown are mean ± SD and are representative of 4 independent experiments. *$P < .05$.

analyzed with Ingenuity Pathway Analysis selecting altered upstream regulators using a cutoff of a P value $< .05$ and an absolute value z score ≥ 2.

Statistics

Plots were generated using GraphPad Prism 5.0 (La Jolla, CA). Unless specified, the Wilcoxon rank-sum (Mann-Whitney) test was used to calculate significance. For evaluation of daily weights and T-cell cytotoxicity, statistical significance was calculated using 2-way analysis of variance (ANOVA), whereas for survival studies the log-rank test was used. Significance is reported as *($P < .05$) and **($P < .001$). P values $< .05$ were considered significant.

Results

Ruxolitinib ameliorates the hematologic manifestations of CpG-induced HLH

Following the repeated engagement of Toll-like receptor 9 by the serial administration of CpG DNA, B6 mice experience activation of the innate immune system and develop many of the cardinal manifestations of HLH, including trilineage cytopenias, hypercytokinemias, and tissue inflammation.[18] Because an HLH-like disease can be induced in wild-type (WT) mice, this model of CpG-induced inflammation has been used to simulate the secondary forms of disease, which are generally not associated with germ line mutations. To determine whether inhibition of JAK signaling would attenuate disease severity, B6 mice were administered PBS or CpG every other day for 9 days (Figure 1A). Beginning on day 4, mice were treated or not with ruxolitinib twice daily by oral gavage. On day 9, animals were euthanized, and organs harvested and examined.

Compared with control PBS-treated mice, CpG-treated animals developed marked splenomegaly as determined by gross visual inspection (Figure 1B) and measurement of the spleen-to-body weight ratio (Figure 1C). CpG-treated animals also developed pancytopenia, including reductions in the white blood cell (WBC) count, hemoglobin (Hgb), red blood cell (RBC) count, and platelet count (Plt; Figure 1D). The reduction in WBC was primarily due to a decrease in the absolute lymphocyte count. Remarkably, treatment of CpG-injected mice with ruxolitinib at a dose previously shown to lessen disease features and prolong survival in a murine model of JAK2-driven myeloproliferative disorder[20] significantly lessened these clinical and laboratory parameters, restoring spleen size, WBC, RBC, Hgb, and Plt count to those observed in control PBS-injected mice (Figure 1D). Of note, the administration of ruxolitinib to control PBS-injected mice had no effect on baseline hematologic parameters (Figure 1D).

Ruxolitinib lowers serum cytokine levels and reduces tissue inflammation in CpG-treated mice

CpG-treated mice exhibit elevated levels of serum cytokines, including IFNγ, which is critical for disease initiation and progression.[18] To examine whether JAK inhibition reduces CpG-induced hypercytokinemia, we measured serum cytokine levels in mice that had or had not received treatment with ruxolitinib. As previously reported, CpG-treated mice developed increased serum IFNγ, IL-6, and IL-12 (Figure 2A). In contrast, these proinflammatory cytokines were significantly lower and reduced to baseline levels in ruxolitinib-treated animals (Figure 2A). Curiously, ruxolitinib treatment of CpG-injected mice did not show lowering of every cytokine, as can be seen by the modest but not statistically significant decrease in the serum level of IL-10 (Figure 2A).

In HLH, activated immune cells infiltrate organs where they cause considerable tissue damage. Given its positive effects on CpG-induced

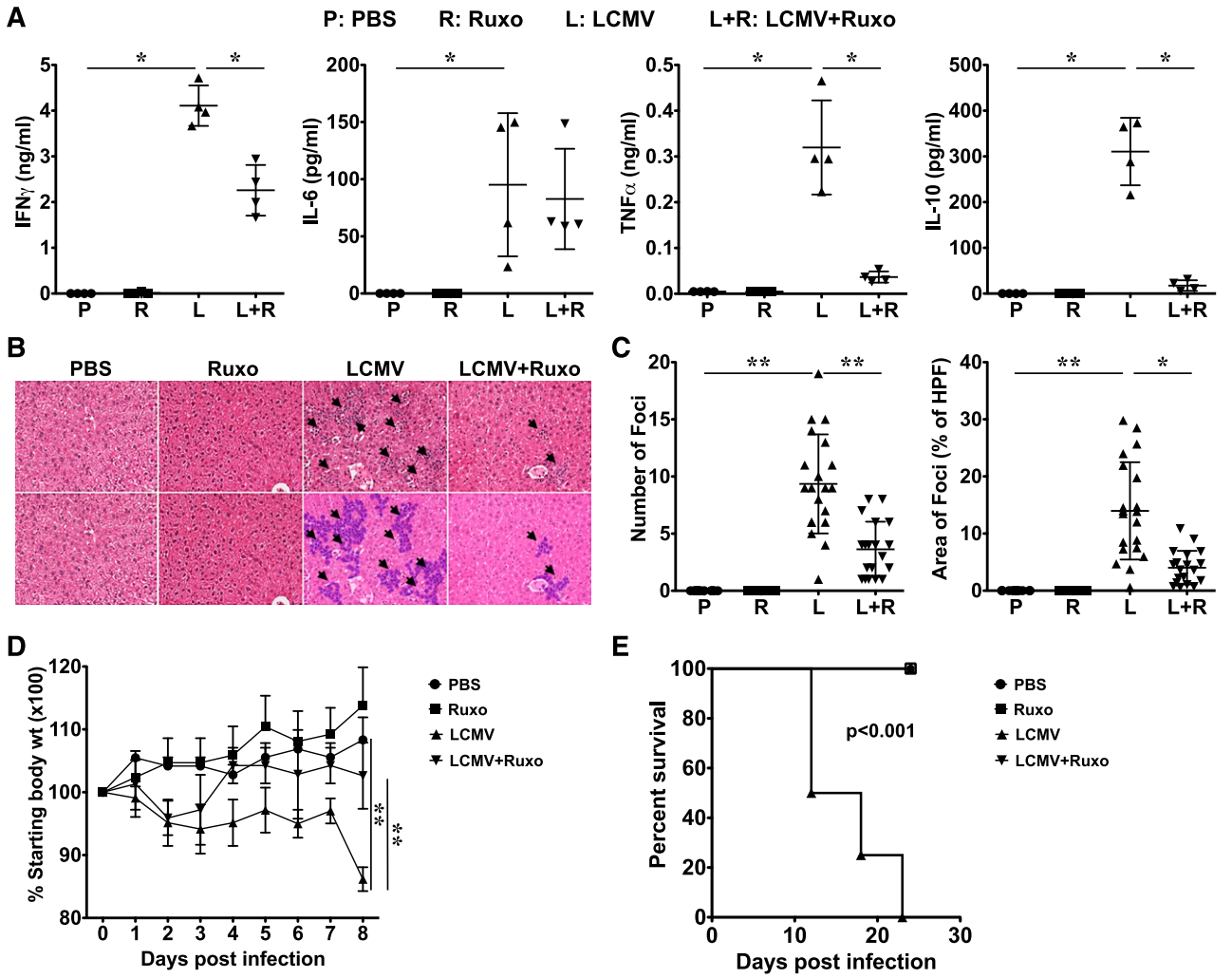

Figure 4. Ruxolitinib treatment reduces LCMV-induced hypercytokinemias and ameliorates liver inflammation. (A) Serum cytokine levels were assessed on days 8 to 10. (B) H&E-stained liver sections demonstrate inflammatory infiltrates (dark purple clusters), indicated by arrows. Representative sections are shown at a magnification of ×20 (top panels) and following computer analysis of inflammatory area (bottom panels). (C) The number of inflammatory foci (left) and percent area occupied by inflammatory foci with respect to the HPF view (right) was determined as in Figure 2. Data shown as mean ± SD are representative of 4 experiments. (D) Daily body weight is depicted as a ratio of the current over initial body weight ×100 with statistical significance determined by 2-way ANOVA. Symbols in panel A represent individual mice in each treatment group; in panel C, they represent the number of, or area encompassed by, inflammatory foci (clusters containing >8 lymphocytes) per ×20 field of view, whereas in panel D they represent the mean daily weight of the animals in each cohort. (E) Overall survival is depicted and statistical significance was determined by the log-rank test. Data in panels D and E are representative of 4 and 2 independent experiments, respectively. *$P < .05$, **$P < .001$.

cytopenia and hypercytokinemia, we next assessed whether JAK1/2 inhibition might ameliorate CpG-induced immunopathology. To do so, we quantified the number and size of inflammatory foci (Figure 2B arrows) in the livers of PBS- or CpG-injected mice that had or had not received treatment with ruxolitinib. Compared with the livers of PBS-treated mice, which had an average of 0.59 ± 0.21 inflammatory foci per HPF, the livers of CpG-treated animals exhibited 5.5-fold more foci (3.28 ± 0.43/HPF), encompassing 1.72% ± 0.05% of the total field of view. Strikingly, this immune infiltration was abrogated by treatment with ruxolitinib, where the number and area were reduced to 0.16 ± 0.37/HPF and 0.05% ± 0.02%, respectively. Again, administration of ruxolitinib to control PBS-injected mice had no effect on basal cytokine levels or tissue histology.

Ruxolitinib lessens the manifestations and enhances survival in LCMV-induced HLH

The primary form of HLH has been modeled using perforin-deficient ($Prf1^{-/-}$) mice, which, like human perforin-deficient patients, exhibit pronounced defects in lymphocyte cytotoxic function. $Prf1^{-/-}$ mice fail to clear infection with LCMV, and instead develop a pathological expansion and activation of $CD8^+$ T cells that secrete a plethora of proinflammatory cytokines.[21,22] To define the therapeutic effects of JAK inhibition in this model of primary HLH, $Prf1^{-/-}$ mice were treated with PBS or infected with 2×10^5 PFU LCMV Armstrong. Beginning on day 4 postinfection, animals were treated or not with ruxolitinib twice daily by oral gavage (Figure 3A). Between days 8 and 10, the peak of the T-cell antiviral immune response, animals were euthanized and the organs harvested. As anticipated, LCMV-infected animals developed splenomegaly, anemia, and thrombocytopenia (Figure 3B-D); however, following treatment with ruxolitinib, these parameters completely normalized. In contrast to CpG-injected B6 mice whose splenic leukocyte count was reduced at day 9, the splenic leukocyte count of LCMV-infected $Prf1^{-/-}$ mice was significantly increased compared with noninfected animals (Figure 3D). Although ruxolitinib treatment normalized the WBC in CpG-injected mice, such treatment had variable effects on the WBC of LCMV-infected

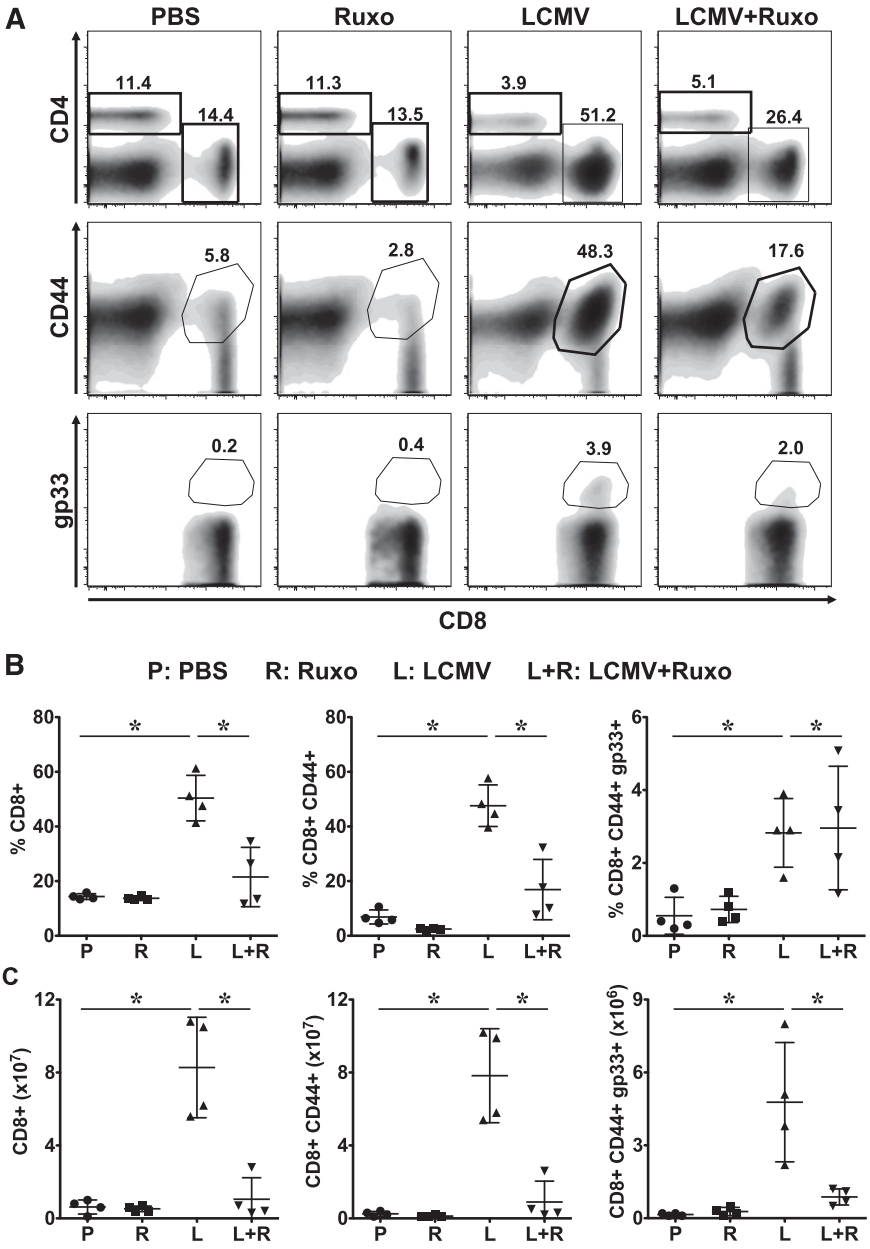

Figure 5. Ruxolitinib reduces the numbers of activated and LCMV-specific CD8$^+$ T cells in LCMV-infected *Prf1*$^{-/-}$ mice. Mice treated with PBS, ruxolitinib, LCMV, and LCMV + ruxolitinib (L+R) were euthanized on day 9 postinfection. Splenocytes were stained using anti-CD4, CD8, CD44 antibodies and fluorochrome-conjugated MHC class I tetramer (D^bgp33). (A) Representative flow cytometric plots showing the percentages of CD4$^+$, CD8$^+$, CD8$^+$CD44$^+$ (top and middle panels, gated on live splenocytes) and CD8$^+$gp33$^+$ (bottom panels, gated on CD8$^+$CD44$^+$ cells) cells from a representative mouse in each group. (B) Percentage and (C) absolute number of splenic CD8$^+$, CD8$^+$CD44$^+$, and CD8$^+$CD44$^+$gp33$^+$ cells. Data are shown as mean ± SD and are representative of 4 independent experiments. *$P < .05$.

mice with some animals showing normalization of WBC, whereas in others it had minimal to no effect.

Compared with CpG-induced disease, the levels of serum IFNγ were 164-fold higher in LCMV-infected *Prf1*$^{-/-}$ mice, with an average concentration of 4.1 ± 0.22 ng/mL (Figure 4A). LCMV-infected mice also exhibited increased serum levels of other proinflammatory cytokines, such as IL-6 and TNF-α (Figure 4A). Consistent with these observations, LCMV-infected mice demonstrated a more pronounced increase in the number (9.4 ± 1/HPF) and area (14% ± 1.9%) encompassed by the inflammatory foci in the liver (Figure 4B arrows). Despite the substantial increase in systemic inflammation, treatment with ruxolitinib significantly attenuated the levels of proinflammatory cytokines such as IFNγ and TNFα (but not IL-6) and reduced the number and size of inflammatory foci (Figure 4A-C). Importantly, ruxolitinib treatment also significantly lessened the profound weight loss induced by LCMV infection (Figure 4D) and it markedly enhanced survival (Figure 4E). Together, these data reveal that treatment with ruxolitinib reduces morbidity and mortality in a therapeutically relevant manner in this model of primary HLH, a severe human immune deficiency.

Ruxolitinib reduces T-cell expansion in LCMV-infected *Prf1*$^{-/-}$ mice

The genetic mutations that underlie primary HLH negatively impact the composition, formation, movement, and release of cytotoxic granules.[1] It is proposed that the resulting inability of T and NK cells to properly lyse infected cells and antigen-presenting cells leads to persistent immunostimulation and uncontrolled proliferation and activation of CD8$^+$ T cells. Consistent with this notion, depletion of CD8$^+$ T cells lessens serum cytokine levels and tissue immunopathology in LCMV-infected *Prf1*$^{-/-}$ mice.[21] To understand how ruxolitinib is ameliorating the T-cell–dependent disease phenotype, we examined whether treatment influenced the number, phenotype, or function of CD8$^+$ T cells in LCMV-infected *Prf1*$^{-/-}$ mice. Following LCMV infection, we observed a significant increase in the frequency and absolute

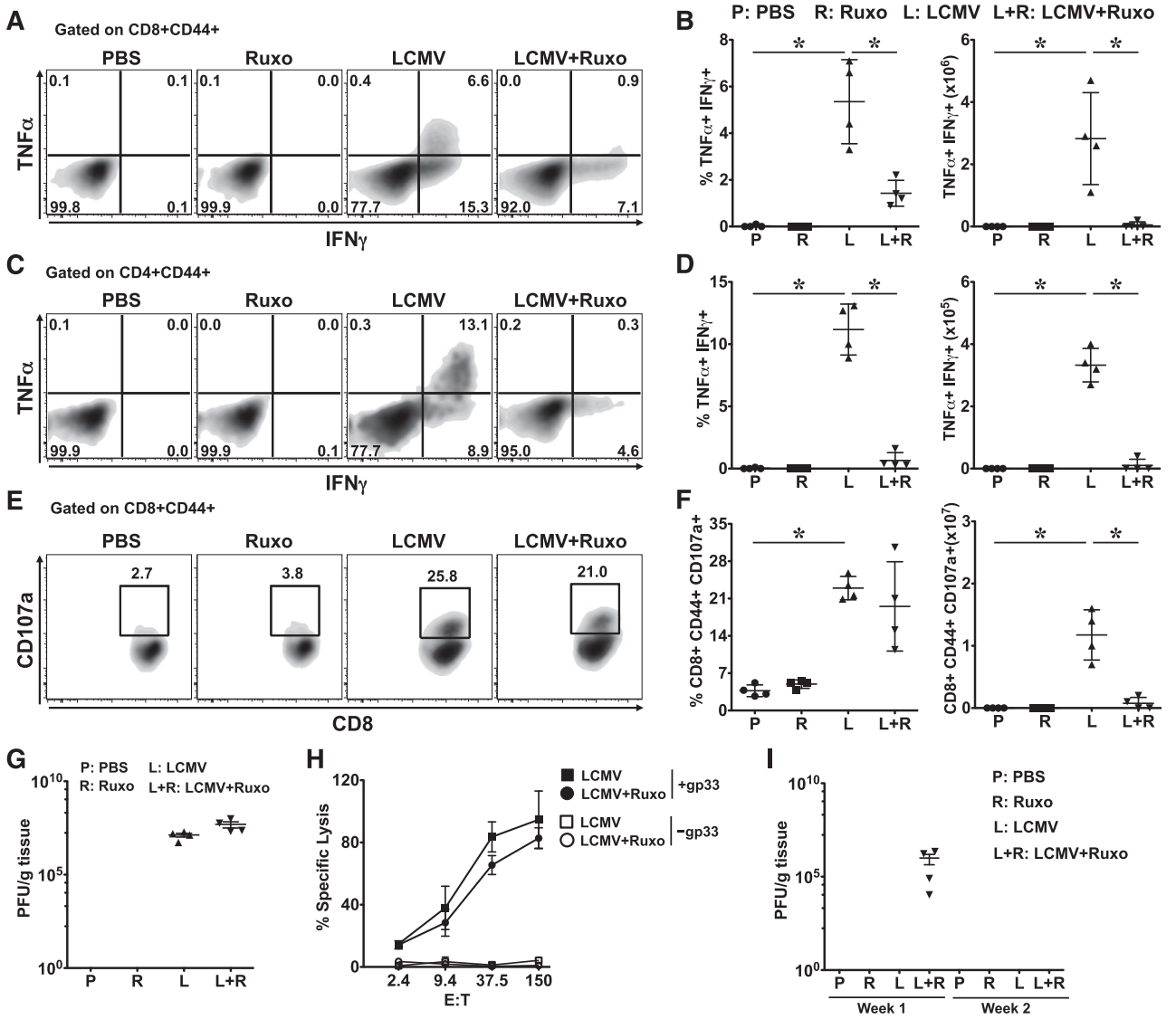

Figure 6. In vivo exposure to ruxolitinib differentially influences T-cell functions. *Prf1*$^{-/-}$ mice were infected with LCMV and treated with ruxolitinib as described. On day 9, splenocytes from these animals were restimulated ex vivo with MHC class I (gp33-41)- or class II (gp61-80)-restricted LCMV peptides. Percentages of CD8$^+$CD44$^+$ (A-B [left]) and CD4$^+$CD44$^+$ (C-D [left]) T cells producing both TNFα and IFNγ, or CD8$^+$CD44$^+$ T cells expressing LAMP1 (CD107a; E-F [left]) were determined by intracellular and surface staining and flow cytometry. Absolute number of CD8$^+$CD44$^+$ and CD4$^+$CD44$^+$ T cells producing both TNFα and IFNγ, and CD8$^+$CD44$^+$CD107$^+$ are shown in panels B, D, and F, respectively (right panels). In panels B, D, and F, data are presented as mean ± SD. (G) Viral titer was determined in the liver samples of *Prf1*$^{-/-}$ mice in each group. (H) EL4 cells were pulsed with 20 μM gp33-41 peptide or left untreated and used as targets in an in vitro cytotoxicity assay. Cytolysis of gp33-loaded (filled symbols) or unloaded (open symbols) EL4 cells by splenic CD8$^+$CD44$^+$ cells of LCMV-infected or LCMV + ruxolitinib–treated (L+R) B6 mice. Specific lysis was determined by ^{51}Cr release and plotted as the mean ± SD. Statistical significance in percent-specific lysis was determined by 2-way ANOVA. (I) Viral titers in the livers of B6 mice on day 8 (week 1) and day 15 (week 2) postinfection. Data in panels A through G and H and I are representative of 4 and 2 independent experiments, respectively. *$P < .05$.

number of total as well as LCMV-specific (gp33 tetramer-positive) splenic (Figure 5) and intrahepatic (supplemental Figure 1, available on the *Blood* Web site) CD8$^+$ T cells, with most of these cells expressing the CD44$^+$ activation marker. Remarkably, treatment with ruxolitinib significantly reduced the percentage and absolute number of CD8$^+$ T cells, including those exhibiting an activated phenotype. Although the frequency of LCMV-specific CD8$^+$ T cells was unchanged following ruxolitinib treatment, the absolute number was reduced as a consequence of the overall reduction in CD8$^+$ T cells.

Ruxolitinib reduces T-cell cytokine production but does not impair degranulation or cytotoxicity

To examine whether exposure to ruxolitinib influenced LCMV-specific T-cell functions, splenocytes from infected or uninfected *Prf1*$^{-/-}$ mice were incubated with or without the major histocompatibility complex (MHC) class I– or II–restricted LCMV peptides gp33-41 and gp61-80, respectively. Five hours later, T cells were stained and assessed for intracellular IFNγ and TNFα, and for evidence of degranulation. Unlike T cells from uninfected mice, a significant proportion of splenic CD8$^+$ (Figure 6A-B) and CD4$^+$ (Figure 6C-D) T cells from LCMV-infected mice simultaneously produced IFNγ and TNFα. Similarly, up to 20% of the CD8$^+$ T cells degranulated as indicated by their increased cell surface expression of LAMP1 (CD107a). Strikingly, cells from LCMV-infected and ruxolitinib-treated animals exhibited reduced production of IFNγ and TNFα (Figure 6A-D), but normal degranulation (Figure 6E-F). Consistent with the latter observation, we observed no increase in viral burden in the spleens or livers of ruxolitinib-treated vs untreated *Prf1*$^{-/-}$ mice (Figure 6G and data not

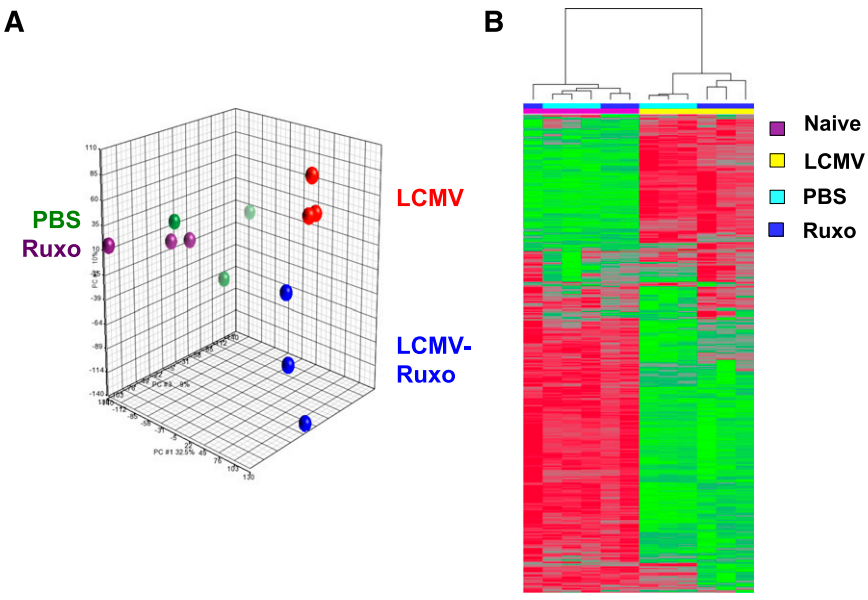

Figure 7. Ruxolitinib treatment inhibits STAT1-dependent gene expression in splenic CD8$^+$ T cells from LCMV-infected *Prf1*$^{-/-}$ mice. TCRβ$^+$ CD8$^+$CD44$^+$ T cells were sort-purified from the spleens of uninfected untreated (PBS), uninfected ruxolitinib-treated (Ruxo), LCMV-infected (LCMV), and LCMV-infected ruxolitinib-treated (LCMV, Ruxo) *Prf1*$^{-/-}$ mice. Sorted T cells were used to isolate RNA and complete complementary DNA microarray analysis. (A) PCA of the unfiltered data set. Each dot represents 1 mouse within each cohort. (B) Unsupervised hierarchical clustering of probe sets filtered on a log2 expression difference of >1.5 (1035 total probe sets). The height of the branches in the dendrogram reflects the distances between samples. Probe sets in green represent upregulated genes, compared with the mean expression; red represents downregulated genes.

shown). Because *Prf1*$^{-/-}$ T cells exhibit no cytotoxic potential, we used WT B6 T cells to evaluate whether ruxolitinib treatment would adversely affect lytic activity. CD8$^+$ T cells were sorted from the spleens of B6 mice that had been infected with LCMV and treated or not with ruxolitinib. T cells were placed in culture with ^{51}Cr-labeled target cells that had or had not been pulsed with gp33 peptide and specific lysis was determined using a ^{51}Cr release assay. In agreement with the degranulation data, both ruxolitinib-exposed and -unexposed B6 CD8$^+$ T cells exhibited robust killing of gp33-pulsed (Figure 6H filled symbols), but not unpulsed (Figure 6H open symbols), target cells. Furthermore, ruxolitinib-treated B6 mice cleared LCMV infection, albeit with a slight delay in kinetics compared with untreated animals (Figure 6I).

Ruxolitinib suppresses STAT1-dependent gene expression in T cells from infected *Prf1*$^{-/-}$ mice

To establish whether ruxolitinib, a potent inhibitor of JAK1 and JAK2, ameliorates HLH by influencing patterns of JAK-STAT–dependent gene expression, we performed gene expression profiling using RNA isolated from splenic CD8$^+$ T cells sorted directly ex vivo from LCMV-infected or uninfected *Prf1*$^{-/-}$ mice that had or had not been treated with ruxolitinib. PCA of the unfiltered data set suggested clustering of the gene expression profiles of CD8$^+$ T cells from uninfected *Prf1*$^{-/-}$ mice, regardless of exposure to ruxolitinib (Figure 7A green vs purple). This is in contrast to infected mice, where ruxolitinib substantially altered gene expression patterns (Figure 7A red vs blue). To examine these patterns in more detail, we used unsupervised hierarchical clustering on probe sets with a fold change >1.5 log2 difference (1035 probe sets). This analysis confirmed that ruxolitinib treatment did not induce dramatic changes in gene expression in naive mice, but it did result in distinct differences in gene expression in treated vs untreated LCMV-infected mice (Figure 7B). To explore the meaning of these differences, we generated the list of genes that were differentially expressed in CD8$^+$ T cells from LCMV-infected *Prf1*$^{-/-}$ mice that had been treated or not with ruxolitinib, using a false discovery rate of 5%. This analysis resulted in a list of 631 genes that we then analyzed for putative upstream regulators of gene expression using Ingenuity Pathway Analysis (Table 1). Consistent with the known mechanism of action of ruxolitinib, we found that *IFNγ*, *STAT1*, and *IRF1* were the top gene regulators predicted to be inhibited in ruxolitinib-treated mice.

Discussion

Despite current treatment approaches, many HLH patients die due to the damaging effects of unbridled inflammation, which is fueled by high systemic levels of proinflammatory cytokines. Because many HLH-associated cytokines signal via the JAK-STAT pathway, we hypothesized that JAK inhibition would diminish inflammation and lessen disease. Indeed, using 2 murine models, we show that the JAK1/2 inhibitor ruxolitinib significantly reduces the manifestations of HLH and, importantly, such treatment also enhances survival. In vivo exposure to ruxolitinib differentially influences CD8$^+$ T-cell functions, as revealed by reduced IFNγ and TNFα production but normal degranulation and cytotoxic function. Collectively, these data highlight the central role for JAK-dependent pathways in HLH and provide proof-of principle that JAK inhibition serves as a viable therapeutic strategy to reverse the life-threatening hyperinflammation that is typical of these disorders.

In several murine HLH models, the preemptive or therapeutic neutralization of IFNγ lessens inflammation.[18,21,23,24] These findings have supported the notion that IFNγ is a driving cytokine in HLH and spurred development of a neutralizing anti-human IFNγ antibody that is currently under investigation (www.clinicaltrials.gov/ct2/show/NCT01818492). However, cytokines other than IFNγ also play important roles in HLH. Such is the case when *Prf1*$^{-/-}$ mice are infected with murine cytomegalovirus, which also elicits significant tissue inflammation. In this model, however, neutralization of TNFα or treatment with IL-18–binding protein (a natural inhibitor of IL-18), and not neutralization of IFNγ, reduces disease severity.[25,26] Notably, IFNγ is not high in all human HLH patients[27,28] and gene expression profiling does not reveal an IFNγ signature in HLH patient peripheral blood mononuclear cells.[29] These latter observations suggest that IFNγ may not always be the driving cytokine in human HLH. Indeed, HLH

Table 1. Ingenuity Pathway Analysis of sorted CD8$^+$ T cells from LCMV-infected *Prf1*$^{-/-}$ mice that were or were not treated with ruxolitinib

Upstream regulator	Activation z score	*P* value of overlap
TREM1	2.53	1.35E-02
TGFB3	2.372	4.31E-02
MAP3K14	2.213	5.38E-03
E2F1	2.083	3.50E-02
MYOCD	2	9.98E-02
IFNG	−3.075	1.92E-07
STAT1	−2.972	2.45E-03
IRF1	−2.514	3.97E-04
IL27	−2.445	7.33E-03
CEBPA	−2.423	1.34E-02
CEBPB	−2.315	5.04E-03
IL13	−2.239	9.16E-06
NOG	−2.219	1.20E-02
EBI3	−2.216	4.32E-03
IL15	−2.064	3.25E-02

patients exhibit high levels of other JAK-dependent cytokines, such as IL-2, IL-6, and macrophage colony-stimulating factor.[30-32] Therefore, JAK inhibition may be more effective than IFNγ as a treatment of HLH. In support of this this notion, we show that ruxolitinib lessens disease and enhances survival, even when administered well after the initiation of CpG- or LCMV-induced immune stimulation.

Proinflammatory responses are typically counterregulated by anti-inflammatory mechanisms such as the production of IL-10. Because IL-10 signals through JAK1,[33] we were concerned that ruxolitinib might interfere with IL-10 signaling, and thereby exacerbate inflammation. Indeed, previous studies show that IL-10 blockade in the CpG model of secondary HLH leads to increased symptom severity.[18] Despite this concern, we did not observe any worsening of HLH manifestations in ruxolitinib-treated animals. Compared with untreated mice, LCMV-infected ruxolitinib-treated *Prf1*$^{-/-}$ animals exhibited diminished serum IL-10 levels and their splenic T cells exhibited fourfold lower levels of *IL-10* transcripts (data not shown). Although this finding could reflect a direct action of ruxolitinib, it might also result from the lower systemic levels of IFNγ, which are known to drive IL-10 production.[34] Thus, the marked fall of IFNγ observed in ruxolitinib-treated mice might bring a concomitant fall in IL-10. Regardless of the mechanism, sustained IL-10 levels appear unnecessary for disease amelioration, as symptoms and survival improved upon ruxolitinib treatment, despite the lower IL-10 levels.

Ruxolitinib has been reported to impair NK[35] and dendritic cell[36] function, and to dampen T-cell responses.[37,38] It thus remained possible that ruxolitinib would suppress immune function, further impair viral clearance, and lead to greater disease severity. However, ruxolitinib treatment did not result in higher viral loads in *Prf1*$^{-/-}$ mice, nor did it affect the frequencies of LCMV-specific CD8 T cells (though the absolute numbers were reduced twofold). Similarly, ruxolitinib treatment of LCMV-infected B6 mice did not appear to impair in vitro T-cell cytotoxic function and only modestly delayed viral clearance. Despite this delay in viral clearance, B6 mice did not develop any overt signs of HLH or worsening of tissue inflammation (Figure 6 and data not shown).

There are several properties of ruxolitinib that make it particularly appealing as a treatment of HLH. Ruxolitinib targets inflammation in a manner distinct from steroids and etoposide. Therefore, ruxolitinib might synergize with these or other agents to more effectively treat the disease. IL-6 levels remain elevated in LCMV-infected *Prf1*$^{-/-}$ mice despite administration of ruxolitinib. Blockade of IL-6 through use of tocilizumab, a monoclonal antibody recognizing the IL-6 receptor, results in rapid reversal of cytokine release syndrome in patients receiving T-cell–based immunotherapies.[39] Therefore, the combination of ruxolitinib with tocilizumab may prove even more beneficial as a therapy for HLH. Ruxolitinib has a short half-life and its effects can be readily titrated.[18,40] Consequently, it should be possible to identify a dose that does not abrogate JAK function, but instead allows for some degree of cytokine signaling. This residual signaling could minimize immune suppression and the subsequent risk for infection. Finally, ruxolitinib is US Food and Drug Administration (FDA) approved and has a well-defined toxicity profile. The clinical translation of this work could thus be accelerated through the use of this agent, which has already been thoroughly tested in children and adults.[41] Together with these properties, our findings support the integration of JAK inhibitors such as ruxolitinib into HLH clinical trials as a novel strategy to counteract pathological cytokine-driven tissue inflammation.

Acknowledgments

The authors gratefully acknowledge Eric Rappaport and Stephen Mahoney from the NAPCORE Facility at The Children's Hospital of Philadelphia for their assistance with the gene expression profiling.

This work was supported by funding from Sean Fischel Connect, the Histiocytosis Association of America (K.E.N.), and the National Institutes of Health, National Institute of Allergy and Infectious Diseases (R21AI113490) (K.E.N.) and National Cancer Institute (K22CA188149) (R.D.).

Authorship

Contribution: R.D., K.V., and L.S. designed and carried out experiments and wrote the manuscript; P.G. and P.T. provided technical assistance; M.K. and E.J.W. helped with viral infections; C.C. and Q.A.A. performed statistical analyses; R.L. provided ruxolitinib and guidance regarding dosing and administration; E.M.B. and S.W.C. helped with the model of CpG-induced HLH and gene expression profiling; and K.E.N. oversaw the project, interpreted data, and, along with E.M.B. and S.W.C., edited the manuscript.

Conflict-of-interest disclosure: The authors declare no competing financial interests.

The current affiliation for L.S. is Biomedical Sciences Graduate Program, The Ohio State University College of Medicine, Columbus, OH.

The current affiliation for is S.W.C. is Autoinflammatory Pathogenesis Unit, National Institute of Arthritis and Musculoskeletal and Skin Diseases, National Institutes of Health, Bethesda, MD.

Correspondence: Kim E. Nichols, St. Jude Children's Research Hospital, 262 Danny Thomas Blvd, Memphis, TN 38105; e-mail: kim.nichols@stjude.org.

References

1. Janka GE. Familial and acquired hemophagocytic lymphohistiocytosis. *Annu Rev Med.* 2012;63:233-246.
2. Canna SW, Behrens EM. Making sense of the cytokine storm: a conceptual framework for understanding, diagnosing, and treating hemophagocytic syndromes. *Pediatr Clin North Am.* 2012;59(2):329-344.
3. Janka GE, Lehmberg K. Hemophagocytic syndromes–an update. *Blood Rev.* 2014;28(4):135-142.
4. Trottestam H, Horne A, Aricò M, et al; Histiocyte Society. Chemoimmunotherapy for hemophagocytic lymphohistiocytosis: long-term results of the HLH-94 treatment protocol. *Blood.* 2011;118(17):4577-4584.
5. Marsh RA, Allen CE, McClain KL, et al. Salvage therapy of refractory hemophagocytic lymphohistiocytosis with alemtuzumab. *Pediatr Blood Cancer.* 2013;60(1):101-109.
6. Lykens JE, Terrell CE, Zoller EE, Risma K, Jordan MB. Perforin is a critical physiologic regulator of T-cell activation. *Blood.* 2011;118(3):618-626.
7. Terrell CE, Jordan MB. Perforin deficiency impairs a critical immunoregulatory loop involving murine CD8(+) T cells and dendritic cells. *Blood.* 2013;121(26):5184-5191.
8. Klinger M, Brandl C, Zugmaier G, et al. Immunopharmacologic response of patients with B-lineage acute lymphoblastic leukemia to continuous infusion of T cell-engaging CD19/CD3-bispecific BiTE antibody blinatumomab. *Blood.* 2012;119(26):6226-6233.
9. Grupp SA, Kalos M, Barrett D, et al. Chimeric antigen receptor-modified T cells for acute lymphoid leukemia. *N Engl J Med.* 2013;368(16):1509-1518.
10. Kiu H, Nicholson SE. Biology and significance of the JAK/STAT signalling pathways. *Growth Factors.* 2012;30(2):88-106.
11. Kontzias A, Kotlyar A, Laurence A, Changelian P, O'Shea JJ. Jakinibs: a new class of kinase inhibitors in cancer and autoimmune disease. *Curr Opin Pharmacol.* 2012;12(4):464-470.
12. Laurence A, Pesu M, Silvennoinen O, O'Shea J. JAK kinases in health and disease: an update. *Open Rheumatol J.* 2012;6:232-244.
13. Villarino AV, Kanno Y, Ferdinand JR, O'Shea JJ. Mechanisms of Jak/STAT signaling in immunity and disease. *J Immunol.* 2015;194(1):21-27.
14. Fleischmann R, Kremer J, Cush J, et al; ORAL Solo Investigators. Placebo-controlled trial of tofacitinib monotherapy in rheumatoid arthritis. *N Engl J Med.* 2012;367(6):495-507.
15. Sandborn WJ, Ghosh S, Panes J, et al; Study A3921063 Investigators. Tofacitinib, an oral Janus kinase inhibitor, in active ulcerative colitis. *N Engl J Med.* 2012;367(7):616-624.
16. Mascarenhas J, Mughal TI, Verstovsek S. Biology and clinical management of myeloproliferative neoplasms and development of the JAK inhibitor ruxolitinib. *Curr Med Chem.* 2012;19(26):4399-4413.
17. Verstovsek S, Mesa RA, Gotlib J, et al. A double-blind, placebo-controlled trial of ruxolitinib for myelofibrosis. *N Engl J Med.* 2012;366(9):799-807.
18. Behrens EM, Canna SW, Slade K, et al. Repeated TLR9 stimulation results in macrophage activation syndrome-like disease in mice. *J Clin Invest.* 2011;121(6):2264-2277.
19. Das R, Bassiri H, Guan P, et al. The adaptor molecule SAP plays essential roles during invariant NKT cell cytotoxicity and lytic synapse formation. *Blood.* 2013;121(17):3386-3395.
20. Kubovcakova L, Lundberg P, Grisouard J, et al. Differential effects of hydroxyurea and INC424 on mutant allele burden and myeloproliferative phenotype in a JAK2-V617F polycythemia vera mouse model. *Blood.* 2013;121(7):1188-1199.
21. Jordan MB, Hildeman D, Kappler J, Marrack P. An animal model of hemophagocytic lymphohistiocytosis (HLH): CD8+ T cells and interferon gamma are essential for the disorder. *Blood.* 2004;104(3):735-743.
22. Brisse E, Wouters CH, Matthys P. Hemophagocytic lymphohistiocytosis (HLH): a heterogeneous spectrum of cytokine-driven immune disorders. *Cytokine Growth Factor Rev.* 2015;26(3):263-280.
23. Pachlopnik Schmid J, Ho CH, Chrétien F, et al. Neutralization of IFNgamma defeats haemophagocytosis in LCMV-infected perforin- and Rab27a-deficient mice. *EMBO Mol Med.* 2009;1(2):112-124.
24. Kögl T, Müller J, Jessen B, et al. Hemophagocytic lymphohistiocytosis in syntaxin-11-deficient mice: T-cell exhaustion limits fatal disease. *Blood.* 2013;121(4):604-613.
25. van Dommelen SL, Sumaria N, Schreiber RD, Scalzo AA, Smyth MJ, Degli-Esposti MA. Perforin and granzymes have distinct roles in defensive immunity and immunopathology. *Immunity.* 2006;25(5):835-848.
26. Chiossone L, Audonnet S, Chetaille B, et al. Protection from inflammatory organ damage in a murine model of hemophagocytic lymphohistiocytosis using treatment with IL-18 binding protein. *Front Immunol.* 2012;3:239.
27. Maruyama J, Inokuma S. Cytokine profiles of macrophage activation syndrome associated with rheumatic diseases. *J Rheumatol.* 2010;37(5):967-973.
28. Yasutomi M, Okazaki S, Hata I, et al. Cytokine profiles in Mycoplasma pneumoniae infection-associated hemophagocytic lymphohistiocytosis [published online ahead or print December 11, 2014]. *J Microbiol Immunol Infect.* doi:10.1016/j.jmii.2014.11.015.
29. Sumegi J, Nestheide SV, Barnes MG, et al. Gene-expression signatures differ between different clinical forms of familial hemophagocytic lymphohistiocytosis. *Blood.* 2013;121(7):e14-e24.
30. Wada T, Muraoka M, Yokoyama T, Toma T, Kanegane H, Yachie A. Cytokine profiles in children with primary Epstein-Barr virus infection. *Pediatr Blood Cancer.* 2013;60(7):E46-E48.
31. Henter JI, Elinder G, Söder O, Hansson M, Andersson B, Andersson U. Hypercytokinemia in familial hemophagocytic lymphohistiocytosis. *Blood.* 1991;78(11):2918-2922.
32. Takada H, Nomura A, Ohga S, Hara T. Interleukin-18 in hemophagocytic lymphohistiocytosis. *Leuk Lymphoma.* 2001;42(1-2):21-28.
33. Mascarenhas J. Selective Janus associated kinase 1 inhibition as a therapeutic target in myelofibrosis. *Leuk Lymphoma.* 2015;56(9):2493-2497.
34. Saraiva M, O'Garra A. The regulation of IL-10 production by immune cells. *Nat Rev Immunol.* 2010;10(3):170-181.
35. Schönberg K, Rudolph J, Vonnahme M, et al. JAK inhibition impairs NK cell function in myeloproliferative neoplasms. *Cancer Res.* 2015;75(11):2187-2199.
36. Heine A, Held SA, Daecke SN, et al. The JAK-inhibitor ruxolitinib impairs dendritic cell function in vitro and in vivo. *Blood.* 2013;122(7):1192-1202.
37. Heine A, Brossart P, Wolf D. Ruxolitinib is a potent immunosuppressive compound: is it time for anti-infective prophylaxis? *Blood.* 2013;122(23):3843-3844.
38. Parampalli Yajnanarayana S, Stübig T, Cornez I, et al. JAK1/2 inhibition impairs T cell function in vitro and in patients with myeloproliferative neoplasms. *Br J Haematol.* 2015;169(6):824-833.
39. Teachey DT, Rheingold SR, Maude SL, et al. Cytokine release syndrome after blinatumomab treatment related to abnormal macrophage activation and ameliorated with cytokine-directed therapy. *Blood.* 2013;121(26):5154-5157.
40. Ganetsky A. Ruxolitinib: a new treatment option for myelofibrosis. *Pharmacotherapy.* 2013;33(1):84-92.
41. Vaddi K, Sarlis NJ, Gupta V. Ruxolitinib, an oral JAK1 and JAK2 inhibitor, in myelofibrosis. *Expert Opin Pharmacother.* 2012;13(16):2397-2407.

2016 127: 1666-1675
doi:10.1182/blood-2015-12-684399 originally published online January 29, 2016

Janus kinase inhibition lessens inflammation and ameliorates disease in murine models of hemophagocytic lymphohistiocytosis

Rupali Das, Peng Guan, Leslee Sprague, Katherine Verbist, Paige Tedrick, Qi Angel An, Cheng Cheng, Makoto Kurachi, Ross Levine, E. John Wherry, Scott W. Canna, Edward M. Behrens and Kim E. Nichols

Blood (print ISSN 0006-4971, online ISSN 1528-0020), is published weekly by the American Society of Hematology, 2021 L St, NW, Suite 900, Washington DC 20036.